CCA-741 532.613
Conference Paper

The Effect of Curvature on Interfacial Tension in Liquid Systems Measured by Homogeneous Nucleation*

*A. E. Nielsen and P. S. Bindra***

Medicinsk-Kemisk Institut, University of Copenhagen, Copenhagen, Denmark

Received November 27, 1972

Interfacial tensions were measured as a function of the curvature of the interface in liquid ternary, two-phase systems at 25 °C. The systems were chosen so that the phase on the concave side of the interface (= the inner phase = the droplet) consisted mainly of one of the components. When this compound is a non-polar or polar, non-hydrogen bonding liquid the interfacial tension is almost independent of curvature, but when the inner phase is a hydrogen bonding liquid the interfacial tension σ varies with the radius of curvature. The experimental method consisted in determining the time taken for a supersaturated solution to become turbid, this time being of the order of 1 millisecond. The following systems were investigated

I (Good solvent)	II (Poor solvent)	III (Precipitate)
methanol	water	benzene
,,	,,	nitrobenzene
,,	,,	1,2-dichlorobenzene
,,	,,	2,4-dichlorophenol
,,	,,	octanoic acid
2-methyl-2-propanol	benzene	water
1-butanol	,,	water

INTRODUCTION

The theory of the effect of curvature on surface tensions and interfacial tensions has been developed by Gibbs[1], Tolman[2], Koenig[3], Kirkwood and Buff[4,5], Hill[6], Kondo and Ono[7], Choi, Jhon and Eyring[9], and Abraham[10–13], and it has been applied to nucleation phenomena by Parlange[14], Nielsen and Sarig[17], and White and Kassner[19]. For nonpolar substances Tolman[2] derived the equation,

$$\frac{\sigma_\infty}{\sigma} = \frac{1}{1 + 2\delta/r} \tag{1}$$

where σ_∞ is the interfacial tension at a flat interface and σ the tension at an interface with radius of curvature, r. The parameter δ is the distance between

* Based on a lecture presented at the *III International Conference on the Chemistry at Interfaces*, Rovinj, Yugoslavia, June 27—30, 1972.

** Present address: Department of Chemistry, The University, Southampton, England.

the Gibbs surface of tension and the equimolar dividing surface. The data of Nielsen and Sarig[17] on nucleation of droplets of tribromomethane in a mixture of water and methanol verified Tolman's equation.

Analyzing all available data on nucleation of droplets from gas phase Abraham[10–13] concluded that the dependence of surface tension on curvature was moderate for nonpolar and for polar, nonhydrogen bonding liquids, but strong for hydrogen bonding liquids. Abraham pointed out that this could be understood on the basis of Good's[20] observation that hydrogen bonding liquids have cosiderably lower surface entropy than other liquids. This supports the assumption that the liquid structure close to the surface of a hydrogen bonding liquid is more ordered than in the interior of the liquid.

If the strongly polar hydrogen bonding molecules form layers at a flat surface this structure will be disturbed when the surface is curved. This change in structure contributes to the Gibbs energy of the droplet and makes the interfacial tension increase with decreasing radius of curvature. This effect has so far only been studied in connection with nucleation from gas phase. As previously reported[17] we have developed an apparatus for the rapid mixing of two liquids and recording the turbidity *versus* time with a time resolution of about 0.1 millisecond. By performing homogeneous nucleation in this apparatus the interfacial tension between the critical nuclei and the mother phase can be determined. In this manner interfacial tensions can be found for many systems where the classical (macroscopic equilibrium) methods do not apply, *e. g.*, solid-liquid interfaces[18] or strongly curved liquid-liquid-interfaces[17].

EXPERIMENTAL

Two stable, ternary solutions A and B (see Fig. 1) are rapidly mixed to form a homogeneous though unstable solution, D, within the solubility gap of the ternary liquid system. This unstable solution subsequently decomposes into the two stable solutions E and F. E and F are the conjugate equilibrium phases connected by the straight line through D. At small supersaturations the rate of homogeneous nucleation is so slow that the transition into two phases is initiated by heterogeneous nucleation. But at high supersaturation the number of homogeneously nucleated droplets (all growing by a diffusion controlled rate) is so large that the turbidity is primarily determined by the combined nucleation-growth kinetics. Details of the

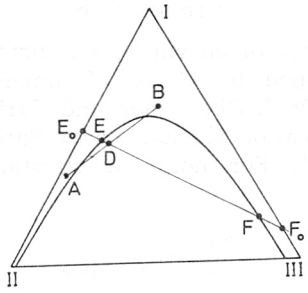

Fig. 1. Triangular phase diagram for the ternary liquid system with components I, II, and III. Liquids I and II are miscible in all proportions, and so are I and III. Liquids II and III are only partially miscible.

By rapid mixing of liquids of the compositions, A and B, an unstable homogeneous mixture D is first formed. This quickly breaks down into two stable phases, E and F, which are in mutual equilibrium. At sufficiently high supersaturations this process is initiated by homogeneous nucleation. As there is a relation between the supersaturation necessary for homogeneous nucleation, and the interfacial tension, the latter may be determined experimentally from the supersaturation. The values found correspond to droplets of the critical size, where the radius of the droplets (and so the radius of curvature of the interface) is of the order, 10—30 Å.

apparatus were described previously.[17] One change was made in the procedure: we did not evacuate the mixing apparatus as this operation turned out to be unnecessary.

THEORY

As the solubilities of the substances precipitated were often quite high the affinity of the processes could not be calculated as $kT \ln S_c$, where $S_c \equiv \equiv c/c_s$, *i. e.* the concentration supersaturation ratio. It was necessary to introduce activity coefficients and use $kT \ln S$, where $S = a/a_s$, *i. e.* the ratio between the activity a in the supersaturated solution and the activity a_s in a solution which is saturated with respect to a macroscopic phase of the precipitating substance. One further complication was that the precipitates in this work were not pure substances but contained the solvent components in equilibrium concentrations. In order to derive the necessary equations we assumed the solutions to be regular[21–23], which is of course not strictly true, but it is assumed to be sufficiently correct for the present purpose. In some of the cases the interfacial tensions measured by the nucleation method agree with the values obtained by classical macroscopic equilibrium methods. In other cases a very marked difference was observed, which is supposed to be caused by the dependence of interfacial tension on droplet size (the curvature of the interface). In order to analyse this effect the necessary equations had to be developed.

Supersaturation in Binary Mixtures

Fig. 2 shows the molar Gibbs energy change ΔG_m of mixing $1-x$ moles of the pure component A, and x moles of the pure component B at constant temperature and pressure to form one mole of mixture. The curve shown has

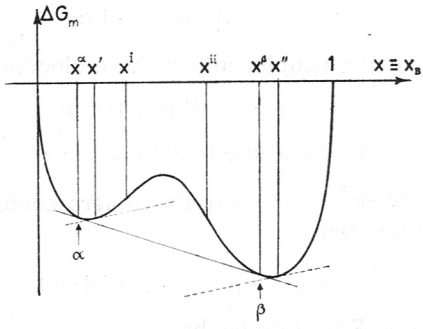

Fig. 2. The molar (or molecular) Gibbs energy of forming a mixture of mole fraction x. The points α and β correspond to coexisting phases. A supersaturated phase of mole fraction, x′, would be in unstable equilibrium with a phase of mole fraction, x″.

two inflexion points, x^i and x^{ii}, and consequently a miscibility gap. The compositions of the two coexisting phases are x^α and x^β where α and β are the two points of tangency with the common tangent. We have of course

$$\mu_A^\alpha = \mu_A^\beta \; ; \; \mu_B^\alpha = \mu_B^\beta \qquad (1); \; (2)$$

A mixture of the composition x', $x^\alpha < x' < x^i$, is metastable, and will not be in equilibrium (stable or unstable) with any macroscopic phase composed of A and B and with the B mole fraction different from x'. (Coexistence is only possible when the two points on the Δ G-curve have a common tangent) But the phase x' may coexist with a critical nucleus of a different composition and

so small that the interfacial Gibbs energy is important. For the formation of a droplet of composition x'', radius r, and interfacial tension σ we have

$$\Delta G = n_A (\mu''_A - \mu'_A) + n_B (\mu''_B - \mu'_B) + A\sigma \tag{3}$$

where $A = 4\pi r^2$. The droplet is in (unstable) equilibrium with the surrounding macroscopic phase (*i. e.*, it is a critical nucleus) when

$$\partial\Delta G/\partial n_A = \partial\Delta G/\partial n_B = 0 \tag{4}$$

or

$$\mu''_A - \mu'_A + \sigma\partial A/\partial n_A + A\partial\sigma/\partial n_A = 0 \tag{5}$$

$$\mu''_B - \mu'_B + \sigma\partial A/\partial n_B + A\partial\sigma/\partial n_B = 0 \tag{6}$$

The terms with $\partial\sigma$ are difficult to estimate. But for a droplet which is in equilibrium with the mother phase the interfacial tension will not vary much with the transfer of a differential amount of one of the components because, according to the Gibbs adsorption law, the component which decreases σ will already be concentrated in the interfase, and the component which increases σ will primarily go to the interior of the phase. We shall therefore neglect the terms with $\partial\sigma$.

As the exact dependencies of the chemical potentials on mole fractions are not known, we will in the following use the formulae valid for regular solutions[21-23]. So we shall assume that the partial molar volumes of the two components are equal and independent of the mole fractions. Consequently

$$\partial A/\partial n_A = \partial A/\partial n_B = \mathrm{d}A/\mathrm{d}n \tag{7}$$

When V is the volume of the droplet and v the molecular volume we have

$$n = n_A + n_B = V/v = 4\pi r^3/3v \tag{8}$$

$$\sigma \mathrm{d}A/\mathrm{d}n = \sigma 8\pi r/(4\pi r^2/v) = 2\sigma v/r \tag{9}$$

The condition for equilibrium between the macroscopic and the microscopic phase can therefore be written

$$\mu''_A - \mu'_A = \mu''_B - \mu'_B = -2\sigma v/r \tag{10}$$

The supersaturation ratio S is defined by

$$-kT \ln S = x_A (\mu''_A - \mu'_A) + x_B (\mu''_B - \mu'_B) \tag{11}$$

It follows that

$$kT \ln S = 2\sigma v/r \tag{12}$$

Using an asterisk for indicating values belonging to the critical nucleus we have

$$r^* = 2\sigma v/kT \ln S \tag{13}$$

$$n^* = \frac{32\pi\sigma^3 v^2}{3(kT \ln S)^3} \tag{14}$$

$$\Delta G^* = \frac{16\pi\sigma^3 v^2}{3(kT \ln S)^2} \tag{15}$$

A system with miscibility gap is far from being an ideal mixture. But if the mutual solubilities are extremely small one may approximate $x'' \approx 1$; $\mu'_A \approx \approx \mu^0_A$; $\mu^\alpha_B = \mu^\beta_B \approx \mu''_B \approx \mu^0_B$; $\mu'_B \approx \mu^\alpha_B + kT \ln (x'/x^\alpha) \Rightarrow$

$$kT \ln S \approx kT \ln (x'/x^\alpha) \equiv kT \ln S_c \tag{16}$$

i. e., the concentration supersaturation ratio.

When the mutual solubilities are appreciable, the use of S_c instead of the correct (activity) supersaturation ratio S may lead to serious errors. For a binary regular solution[21-23]

$$\mu_A = kT (\ln x_A + \omega x_B^2) \tag{17}$$

$$\mu_B = kT (\ln x_B + \omega x_A^2) \tag{18}$$

where ω is a constant.

The compositions of the coexisting phases are given by

$$x^\alpha + x^\beta = 1 \tag{19}$$

$$(x^\beta - x^\alpha)\, \omega = \ln (x^\beta/x^\alpha) \tag{20}$$

The composition of the critical nucleus (x'') in unstable equilibrium with a phase of composition x' is given by (10) or

$$\ln x'_A + \omega x'^2_B - (\ln x''_A + \omega x''^2_B) = \ln x'_B + \omega x'^2_A - (\ln x''_B + \omega x''^2_A) \tag{21}$$

Rearranging, using $x''^2_A - x''^2_B = 1 - 2x''_B$, and defining

$$F(x, \omega) \equiv \ln \frac{x}{1-x} + \omega (1 - 2x) \tag{22}$$

eq. (21) may be written

$$F(x', \omega) = F(x'', \omega) \tag{23}$$

The supersaturation ratio S can now be expressed by means of x' and x''

$$\ln S = \frac{\mu'_B - \mu''_B}{RT} = \ln \frac{x'}{x''} + \omega [(1-x')^2 - (1-x'')^2] \tag{24}$$

In the calculations we treated the ternary mixtures along a tie line, and its linear extensions (E_0F_0 on Fig. 1) formally as binary mixtures of the binary pseudocomponents whose compositions correspond to points E_0 and F_0 on Fig. 1. The supersaturation ratio was determined from x^α and x',

$$x^\alpha \equiv \frac{E_0E}{E_0F_0} \tag{25}$$

$$x' \equiv \frac{E_0D}{E_0F_0} \tag{26}$$

The constant ω was calculated by means of

$$\omega = \frac{\ln (1/x^\alpha - 1)}{1 - 2x^\alpha} \tag{27}$$

which follows from (19) and (20). Eq. (27) was used even if the empirical data

did not obey (19). The B-mole fraction x'' was calculated from ω and x' by means of (23), and finally S was found by inserting x' and x'' in (24).

The calculations were carried out for each individual experiment by means of a programmed electronic calculator. The correct value of S (assuming that the solutions are regular) can also be found from the concentration supersaturation ratio $S_c \equiv x'/x^{\alpha}$ by applying the correction factor $(\log S)/(\log S_c)$. This factor is plotted as a function of $\log S_c$ for a series of values of x^{α} in Fig. 3.

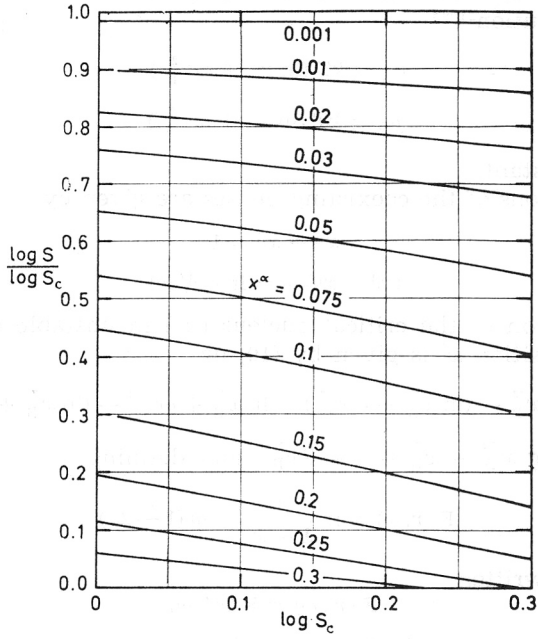

Fig. 3. Diagram for correcting the concentration supersaturation ratio S_c into the activity supersaturation ratio S for liquid mixtures assumed to be regular.

Interfacial Tension

According to the theory of homogeneous nucleation, assuming that the interfacial tension σ is a constant, the Gibbs energy change in formation of a spherical critical nucleus is[15-16]

$$\Delta G^* = \frac{(16\,\pi/3)\ v^2\,\sigma^3}{(kT \ln S)^2} \qquad (28)$$

If the nuclei formed grow by a rate controlled by the diffusion through the surrounding supersaturated solution, the amount precipitated varies with time according to[15,16]

$$\frac{c_0 - c_t}{c_0} = (t/t_1)^{5/2} \qquad (t \ll t_1) \qquad (29)$$

where c_0 = the initial concentration, c_t = concentration at time t, and t_1 is a characteristic constant. It is approximately equal to the half-time, and to the empirically observed induction period. From theory it is derived that

$$t_1 = \frac{v^{2/3}}{2\, x_0^{1/5}\, D} \exp \frac{2\,\Delta G^*}{5\, kT} \tag{30}$$

where x_0 is the mole fraction, and D the diffusion coefficient. Combining equations (28) and (30) we get

$$\sigma^3 = \frac{15}{32\,\pi\, v^2} \left[\ln \frac{2\, x_0^{1/5}\, D\, t_1}{v^{2/3}} \right] (kT)^3\ (\ln S)^2 \tag{31}$$

The radius of the critical nucleus is

$$r^* = \frac{2\, v\, \sigma}{kT \ln S} \tag{32}$$

From (28) and (32) follows

$$(r^*)^2\, \sigma = \frac{3\,\Delta G^*}{4\,\pi} \tag{33}$$

Experimental conditions will often secure that the range of t_1-values is rather limited, and the same is often true for v, $x_0^{1/5}$, and D. For a series of similar experiments ΔG^* will therefore often be roughly constant.

In the experiments reported here we usually have $\Delta G^* \approx 32\, kT = 0.13$ aJ $= 1{,}3 \times 10^{-19}$ J. By varying the composition of the (binary) solvent we were able to change σ and r^* within wide limits for a given precipitating substance. A plot of σ *vs.* $(r^*)^{-2}$ is a straight line because of eq. (33). This does not prove, however that σ is inversely proportional to r^2 in a solution of given composition, because the variation of σ and r found in the experiments are both due to the variation of the solvent.

Any dependence of σ on r at constant concentrations we shall express by means of the equation

$$\sigma = \sigma_\infty\, \mathrm{f}\,(r) \tag{34}$$

where σ_∞ is the value of σ at a plane interface. It is in general possible to measure σ_∞ by classical methods — we used the drop weight method. If it is possible to perform precipitations with homogeneous nucleation followed by diffusion controlled growth it is possible to measure σ at the critical value of $r(r = r^*)$ but, unfortunately, not over a range of r-values. If σ varies with r, σ cannot be calculated from experimental data by means of (31). But we shall define the apparent value, σ_a, by

$$\sigma_a^{\,3} \equiv \frac{3\,\Delta G^*\,(kT \ln S)^2}{16\,\pi\, v^2} = \frac{15}{32\,\pi\, v^2} \left[\ln \frac{2\, x_0^{1/5}\ D\, t_1}{v^{2/3}} \right] (kT)^3\, (\ln S)^2 \tag{35}$$

In order to derive the correction factor σ/σ_a we consider the equation for the Gibbs energy of droplet formation

$$\Delta G = -\, nkT \ln S + A\sigma \tag{36}$$

where

$$n = 4\,\pi\, r^3/3\, v \tag{37}$$

$$A = 4\,\pi\, r^2 \tag{38}$$

i. e.,

$$\Delta G = -\, \frac{4\,\pi\, kT \ln S}{3\, v}\, r^3 + 4\,\pi\,\sigma\, r^2 \tag{39}$$

The condition for phase equilibrium between the droplet and the solution is

$$d\Delta G/dr = 0 \tag{40}$$

which gives

$$kT \ln S = \left(\frac{2\sigma}{r} + \frac{d\sigma}{dr}\right) v \tag{41}$$

Introducing f from eq. (34), (41) becomes

$$kT \ln S = \frac{2 v \sigma_\infty}{r}\left[f + \frac{r}{2}\left(\frac{df}{dr}\right)\right] \tag{42}$$

or

$$r = \frac{2 v \sigma_\infty}{kT \ln S}\, g \tag{43}$$

where

$$g \equiv f + \frac{r}{2}\left(\frac{df}{dr}\right) \tag{44}$$

Inserting r through (37) and (38) into (36) there follows

$$\Delta G^* = \frac{16 \pi v^2 \sigma_\infty^3}{3 (kT \ln S)^2}\, g^2 h \tag{45}$$

where

$$h \equiv 3 f - 2 g = f - r \cdot \frac{df}{dr} \tag{46}$$

Elimination of ΔG^* from (35) and (45) gives

$$\frac{\sigma_a}{\sigma_\infty} = (g^2 h)^{1/3} \tag{47}$$

By means of (34) this leads to

$$\frac{\sigma}{\sigma_a} = \frac{f}{(g^2 \cdot h)^{1/3}} \tag{48}$$

If we define the apparent radius of the critical droplet by

$$r_a \equiv \frac{2 v \sigma_a}{kT \ln S} \tag{49}$$

we have

$$\frac{r}{r_a} = \frac{\sigma_\infty\, g}{\sigma_a} = \left(\frac{g}{h}\right)^{1/3} \tag{50}$$

As an example of the fuction, f, we may take the Tolman[2] equation

$$\frac{\sigma}{\sigma_\infty} = \frac{1}{1 + 2\delta/r} \qquad (\equiv f) \tag{51}$$

Application of the equations derived above gives

$$g = \frac{1 + 3\delta/r}{(1 + 2\delta/r)^2} \tag{52}$$

$$h = \frac{1}{(1 + 2\,\delta/r)^2} \tag{53}$$

$$\frac{\sigma_a}{\sigma_\infty} = \frac{(1 + 3\,\delta/r)^{2/3}}{(1 + 2\,\delta/r)^2} \tag{54}$$

$$\frac{\sigma}{\sigma_a} = \frac{1 + 2\,\delta/r}{(1 + 3\,\delta/r)^{2/3}} \tag{55}$$

$$\frac{r}{r_a} = (1 + 3\,\delta/r)^{1/3} \tag{56}$$

When σ_∞, σ_a, and r_a are known from experiments, δ/r may be found from (54), σ from (55), r from (56), and δ from (51).

Two other types of dependence of σ on r shall be discussed. If

$$\frac{\sigma}{\sigma_\infty} = f \equiv e^{a/r} \tag{57}$$

we find

$$g = e^{a/r}\,(1 - a/2r) \tag{58}$$

$$h = e^{a/r}\,(1 + a/r) \tag{59}$$

$$\frac{\sigma_a}{\sigma_\infty} = e^{a/r}\,[(1 - a/2r)^2\,(1 + a/r)]^{1/3} \tag{60}$$

$$\frac{\sigma}{\sigma_a} = [(1 - a/2r)^2\,(1 + a/r)]^{-1/3} \tag{61}$$

$$\frac{r}{r_a} = \left(\frac{1 - a/2r}{1 + a/r}\right)^{1/3} \tag{62}$$

And if

$$\frac{\sigma}{\sigma_\infty} = f \equiv 1 + a/r \tag{63}$$

we find

$$g = 1 + a/2r = (f + 1)/2 \tag{64}$$

$$h = 1 + 2\,a/r = 2\,f - 1 \tag{65}$$

$$\frac{\sigma_a}{\sigma_\infty} = [(1 + a/2r)^2\,(1 + 2\,a/r)]^{1/3} = [(f + 1)^2\,(2\,f - 1)/4]^{1/3} \tag{66}$$

$$\frac{\sigma}{\sigma_a} = \frac{1 + a/r}{[(1 + a/2r)^2\,(1 + 2\,a/r)]^{1/3}} = \frac{f}{[(f + 1)^2\,(2\,f - 1)/4]^{1/3}} \tag{67}$$

$$\frac{r}{r_a} = \left(\frac{1 + a/2r}{1 + 2a/r}\right)^{1/3} = \left(\frac{f + 1}{4\,f - 2}\right)^{1/3} \tag{68}$$

If we vrite the Tolman equation

$$\frac{\sigma}{\sigma_\infty} = \frac{1}{1 - a/r} \tag{69}$$

where $a = -2\delta$ it becomes easier to compare the three dependencies. We shall be interested both in positive and negative values of a.

In Fig. 4 the three examples of f(r) are plotted as a function of the dimensionless parameter r/a. In Fig. 5 $f(r)$ is plotted as a function of the apparent value σ_a divided by σ_∞.

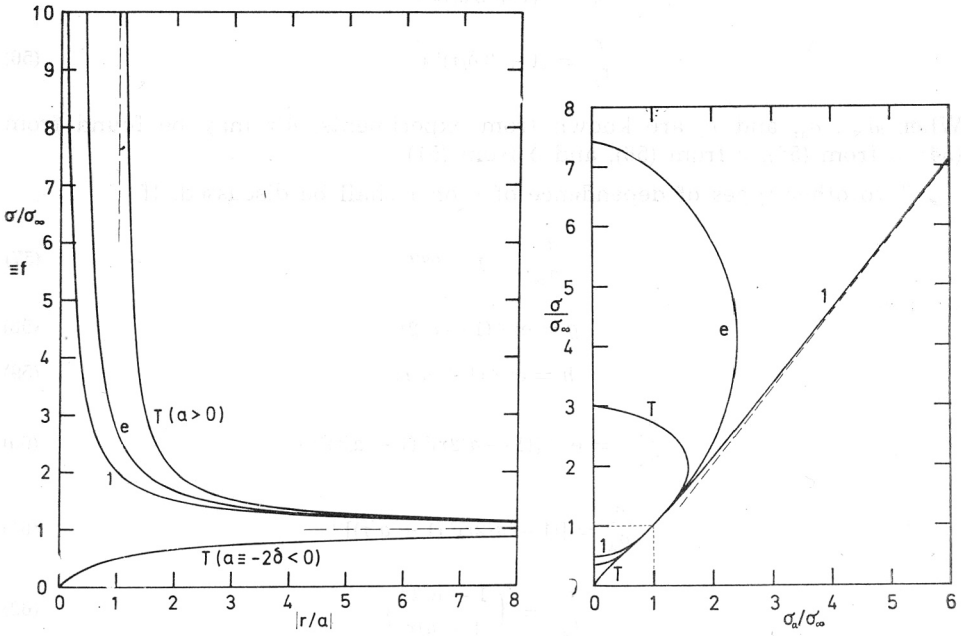

Fig. 4. Theoretical curves for the dependence of the interfacial tension, σ, on radius of curvature. The curves marked T follow the Tolman equation (51) with a = — 2 δ. The other curves correspond to eq. (57) and (63).

Fig. 5. The ratio between the interfacial tension σ at a certain curvature and the values σ_∞ at a plane interface as a function of the ratio between the »apparent value« σ_a of σ from nucleation measurements, and σ_∞. The curves are calculated from the theoretical expressions eq. (51), (57), and (63).

From Fig. 5 we see that for the Tolman equation (51) or (69) and for the exponential equation (57) there is an upper limit to the possible values of σ_a/σ_∞, and below this limit there are two corresponding values of σ. The limiting values of σ_a/σ_∞ are $4^{1/3} = 1.5874$ and $e^{\sqrt{2}}[1/2(\sqrt{2}-1)]^{1/3} = 2.4336$, respectively. Only values of σ/σ_∞ on the lower branch of the curves correspond to critical nuclei.

The values on the upper branch correspond to equating the experimental values of ΔG^* to a minimum on the curve, ΔG *versus* r. See Fig. 6.

Fig. 7. gives the correction factor σ/σ_a to be applied to the apparent value σ_a in order to obtain the correct value σ. Fig. 7 is a simple transformation of Fig. 5.

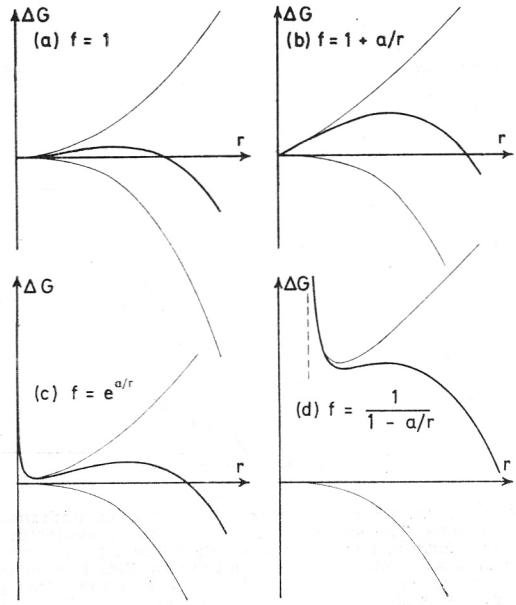

Fig. 6. $\triangle G$ for formation of a droplet with radius, r, in a supersaturated solution. $\triangle G = -n\,kT \ln S + A\,\sigma = -K_1 r^3 + K_2 r^2 f(r)$. In each of the four diagrams the lowest and the uppermost curve are $-K_1 r^3$ and $K_2 r^2 f(r)$, respectively. The middle curve (drawn in a heavy line) is $\triangle G$. (a) $f = 1$, $K_2 r^2 f(r) \sim r^2$, *i. e.* the classical case of constant σ. (b) $f = 1 + a/r$; $K_2 r^2 f(r) \sim ar + r^2$. (c) $f = e^{a/r}$; $K_2 r^2 f(r) \sim r^2 e^{a/r}$; when $\triangle G$ has a maximum (as in the case shown) it has a minimum as well. For a certain value of S the two extrema meet, and for large S-values there are no extrema. (d) $f = 1/(1 - a/r)$, *i. e.* the Tolman equation (with $a = -2\delta$); $K_2 r^2 f(r) \sim r^2/(1 - a/r) = r^3/(r - a)$; when $\triangle G$ has a maximum it has a minimum as well.

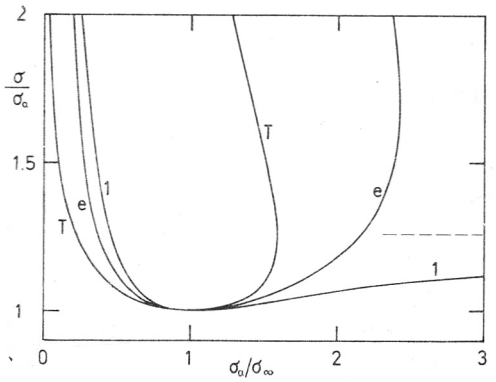

Fig. 7. A plot of σ/σ_a *versus* σ_a/σ_∞ (see Fig. 5). The ordinate is the »correction factor« to be applied to experimental values, σ_a, in order to obtain the correct values, σ.

RESULTS

Figs. 8 to 14 are the triangular phase diagrams at 25 °C for the ternary systems investigated. In all cases one of the pairs of components has a miscibility gap. In the system with 1-butanol two of the component pairs have miscibility gaps, but this does not disturb the method used. The straight lines within the figures are tie lines connecting points corresponding to two phases that may

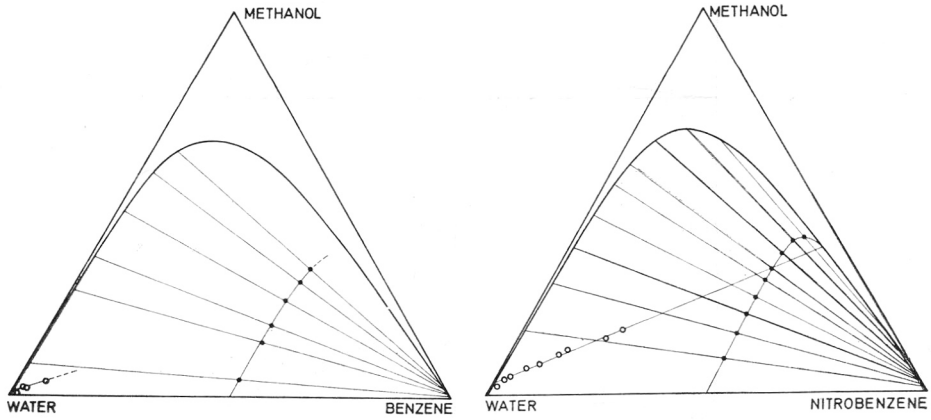

Fig. 8. The triangular phase diagram for the ternary liquid system methanol—water—benzene. The coordinates are volume fractions. The straight lines are tie lines connecting points corresponding to phases that coexist at equilibrium. For benzene—methanol is a good solvent, and water is a poor solvent. By making mixtures as explained in the legend of Fig. 1, a precipitate is formed that consists of practically pure benzene. Concerning the black and the white points, see Fig. 9. The temperature is 25 °C for all the phase diagrams, Fig. 8 to 14.

Fig. 9. The phase diagram for the system, methanol—water—nitrobenzene. The black points are the midpoints of the tie lines. They form a curve which terminates in the critical miscibility-point. Unfortunately the curve bends strongly close to the critical point. This makes the extrapolation uncertain. The white points are plots of one of the triangular coordinates of one of the endpoints of a tie line versus one of the other coordinates of the other endpoint of the same tie line. These »mixed coordinates« points extrapolate along an almost straight line to the critical point.

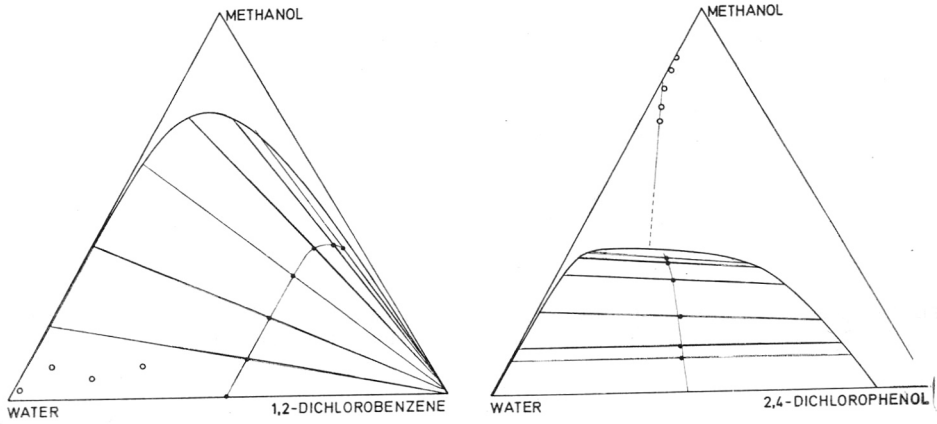

Fig. 10. Phase diagram for methanol—water—1,2-dichlorobenzene.

Fig. 11. Phase diagram for methanol—water—2,4-dichlorophenol.

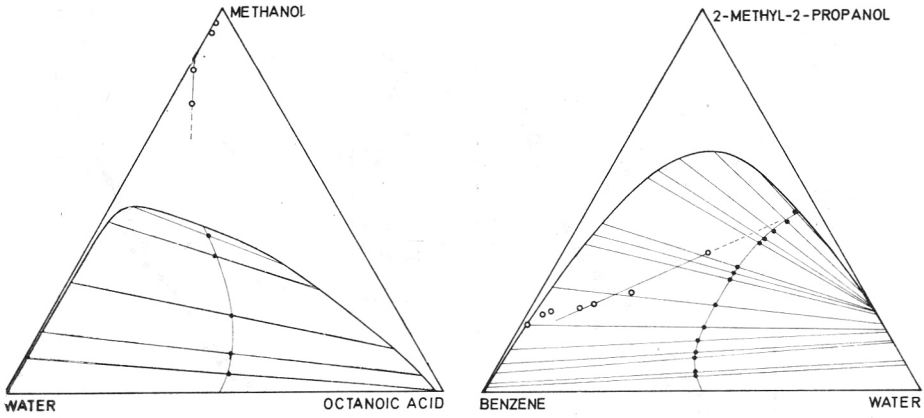

Fig. 12. Phase diagram for methanol—water—octanoic acid (caprylic acid, $CH_3(CH_2)_6COOH$).

Fig. 13. Phase diagram for 2-methyl-2-propanol [tertiary butyl alcohol, $HOC(CH_3)_3$]—benzene—water.

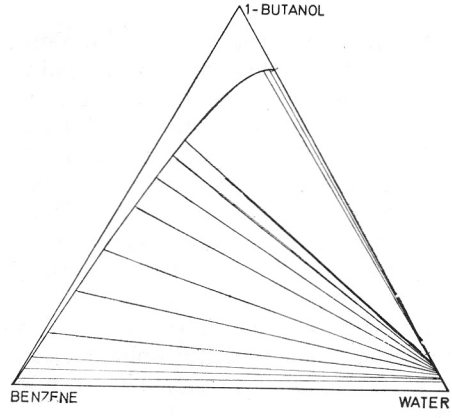

Fig. 14. Phase diagram for 1-butanol [primary butyl alcohol, $CH_3(CH_2)_3OH$]—benzene—water. The presence of a second miscibility gap between the precipitant (water) and the »good solvent« (1-butanol) does not influence the principles of the method.

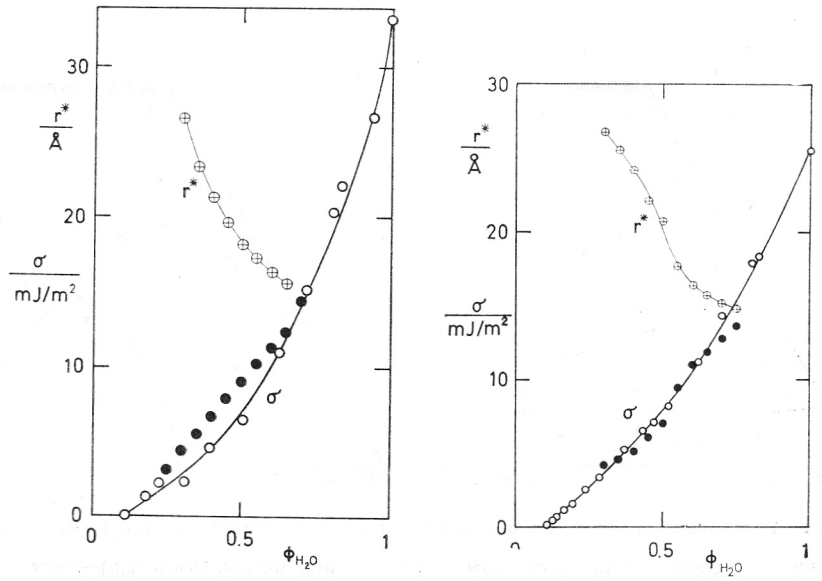

Fig. 15. The interfacial tensions of the two-phase system methanol—water—benzene. One phase consists of practically pure benzene, and the other phase is a saturated solution of benzene in a mixture of methanol and water. By varying the water volume fraction ϕ_{H_2O} the solubility of benzene is changed from complete miscibility to an extremely small value. The white points correspond to the macroscopic value at a plane interface, measured by a classical method, and the black points correspond to the nucleation method. There is a good agreement between the results of the two methods except for an interval in the middle of the range investigated. We have no further comments on this deviation. The circles with crosses show the radius of the critical nuclei as a function of ϕ_{H_2O}.

Fig. 16. The interfacial tensions, and the critical radius as a function of the water volume fraction, for the systems methanol—water—nitrobenzene. The diagram is analogous to Fig. 15. The agreement between the two methods is complete, which seems to indicate that (a) the nucleation method of »microtensiometry« works satisfactorily and (b) [if (a) is agreed on] that the interfacial tension of nitrobenzene droplets in a saturated solution of nitrobenzene in the mixed solvent, methanol + + water, does not depend on curvature when $r > 15$ Å.

coexist. A curve has been drawn through the midpoints of the tie lines. This curve has one end point in the critical miscibility point.

The interfacial tensions found are given in Figs. 15 to 21. In each of the figures white circles show results obtained by the classical drop weight method, where the curvature of the interface is so small that the value obtained may be regarded as the interfacial tension of a macroscopic, plane interface. Black circles are data obtained by the nucleation method described above. The ordinates are interfacial tensions and the abscissae are water volume fractions (calculated from the volumes of the pure components) in the supersaturated homogeneous solution in which nucleation starts. The temperature was always close to 25 °C, and the precipitate consisted in all cases of liquid spherical droplets. This was also true for 2,4-dichlorophenol, (melting point + 45 °C) which precipitated as a supercooled liquid. The droplets did not crystallize until after coagulation.

In all cases the interfacial tensions are relatively small close to the critical miscibility point and increase monotonically as the volume fraction of the poor solvent is increased. In some of the systems the two tensiometric methods (the »nucleation« and the »macroscopic« method) give results that agree within the experimental errors. The agreement is best for nitrobenzene. With benzene

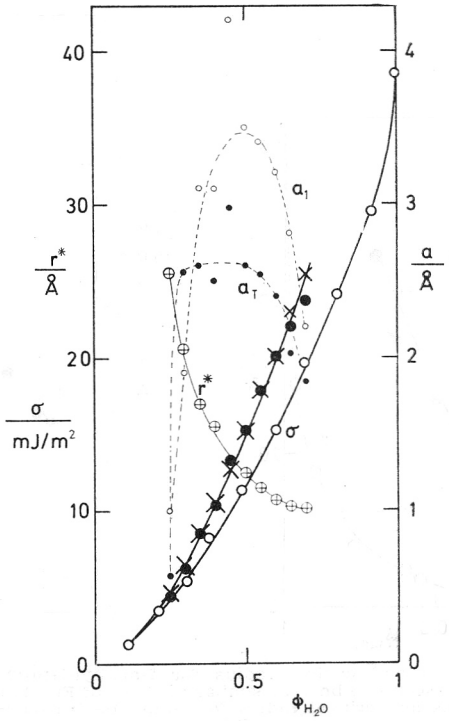

Fig. 17. Interfacial tension and critical radius for the system methanol—water—1,2-dichlorobenzene. Large circles (white, black, and with crosses) have the same meaning as in Fig. 15. The ordinates of the small circles are the values of parameter a in $f_1 \equiv 1 + a/r$ (small white circles) and in $f_T \equiv 1\,(1 - a/r)$ (small black circles). The last equation gives the more constant value of a, *i. e.* the Tolman equation is the better one of the two. Using $a = 2.6$ Å ($\delta = -1.3$ Å) and the experimental values of r and σ_∞ in Tolman's equation the σ-values plotted as large crosses were obtained. They agree with the experimental values σ_a.

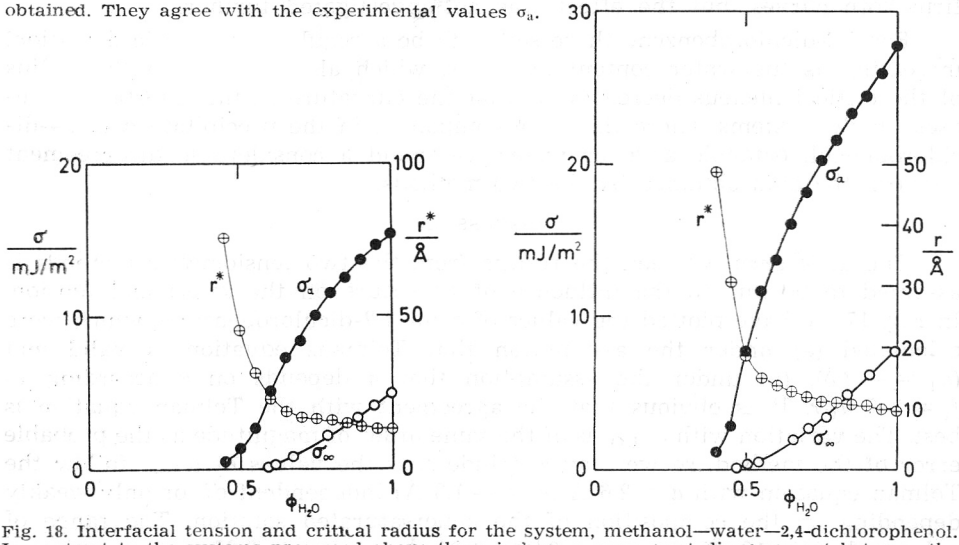

Fig. 18. Interfacial tension and critical radius for the system, methanol—water—2,4-dichlorophenol. In contrast to the systems presented above there is here a very great disagreement between the results of the two methods for liquids of approximately the same composition, which seems to indicate that the interfacial tension depends strongly on the radius of curvature. Because the nuclear interfacial tensions were calculated by means of an equation derived under the assumption that σ is independent of r, their values are apparent and the curve is denoted σ_a.

Fig. 19. Interfacial tensions and critical radius for methanol—water—octanoic acid. The system is very similar to that of Fig. 18.

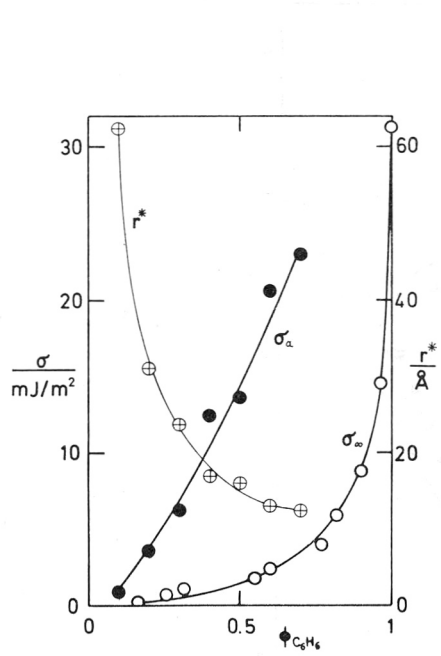

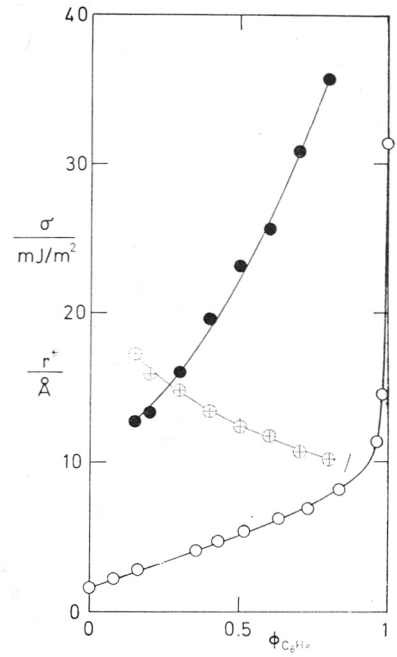

Fig. 20. Interfacial tensions and critical radius for 2-methyl-2-propanol—benzene—water. The system seems to be very similar to those of Fig. 18 and 19.
Fig. 21. Interfacial tensions and critical radius for 1-butanol—benzene—water. Closely similar to Fig. 20.

we found a seemingly irregular deviation in the middle range of concentrations, but agreement in both extreme ends. Repeated measurements seemed to confirm both curves, but the effect was not investigated further.

For 1,2-dichlorobenzene there seems to be a regular, systematic deviation, increasing as the water content increases, which also means that the radius of the critical nucleus decreases, or that the curvature of the interface increases. In the systems where the main component in the precipitate was 2,4-dichlorophenol, octanoic acid, or water we found a considerable disagreement between the data obtained by the two methods.

DISCUSSION

The difference between the results from the two tensiometric methods is assumed to be due to the influence of curvature on the interfacial tension. In Fig. 17 we have plotted the values of a for 1,2-dichlorobenzene, which were calculated (a) under the assumption that Tolmans equation is valid and ($a_T = -2\,\delta$), (b) under the assumption that σ depends on r according to $f_1 = 1 + a_1/r$. It is obvious that the agreement with the Tolman equation is best. The variation with φ_{H_2O} is of the same order of magnitude as the probable error of the method, so we may conclude that the values of σ/σ_∞ follow the Tolman equation with $a = 2.6$ Å ($\delta = -1.3$ Å) independent of, or only weakly depending on the composition of the supersaturated solution. The range of values of r^* is 10 Å at $\varphi_{H_2O} = 0.70$ to 25 Å at $\varphi_{H_2O} = 0.25$.

In a previous paper on the nucleation of tribromomethane it was concluded that the data agreed with the Tolman equation with $\delta = 2.4$ Å ($a = -5.8$ Å).

On the basis of the results with tribromomethane, benzene, nitrobenzene, and 1,2-dichlorobenzene we conclude that the interfacial tensions of nonpolar and of polar, but not hydrogen bonding liquids precipitated from a mixture of water and methanol do not depend strongly on the radius of curvature in the range of radii, 15—25 Å, and when a dependence may be observed it follows the Tolman equation with a positive or a negative value of δ of the order of a molecular diameter.

In four of the systems investigated the difference between the apparent value, σ_a, from nucleation measurements and the value, σ_∞ from macroscopic measurements was very large. In these four systems the main component was 2,4-dichlorophenol, octanoic acid, water, and water respectively. In Fig. 22 we have plotted the ratio σ_a/σ_∞ as a function of the apparent critical radius.

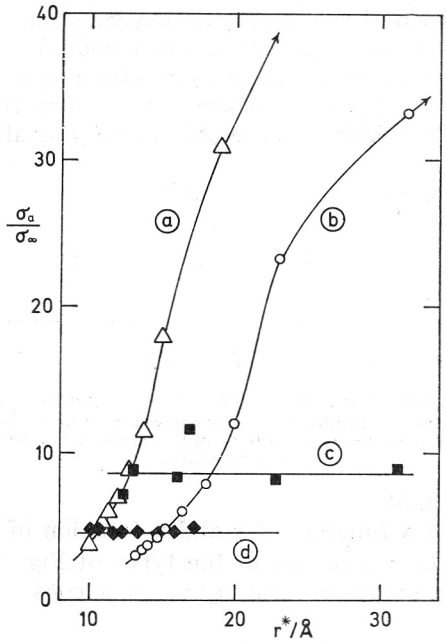

Fig. 22. The ratio between the apparent interfacial tension at the critical radius r^* and the macroscopic interfacial tensions as a function of r^*. *(a)* octanoic acid from methanol + water; *(b)* 2,4-dichlorophenol from methanol + water; *(c)* water from 2-methyl-2-propanol + benzene; *(d)* water from 1-butanol + benzene.

When the main component in the precipitate is water, the ratio σ_a/σ_∞ is constant in the range investigated ($r <$ *ca.* 30 Å). If σ depends on the radius of curvature, r, and the concentration, c, according to

$$\sigma = f(r) \cdot \sigma_\infty (c) \tag{70}$$

the equations (47) to (50) derived above are valid for σ_a/σ_∞ *etc.*, because f being independent of c, g and h as defined by equations (44) and (46) will also be independent of c.

From equations (44), (46), and (47) follows that

$$(\sigma_a/\sigma_\infty)^3 = \left(f + \frac{r}{2}\frac{df}{dr}\right)^2 \left(f - r\frac{df}{dr}\right) = f^3 - 3/4\left(r\frac{df}{dr}\right)^2 f - 1/4\left(r\frac{df}{dr}\right)^3 \tag{71}$$

One of the solutions to the differential equation (71) in an interval where σ_a/σ_∞ = a constant $\equiv f_0$ is $f = f_0$. When this is the case also $\sigma/\sigma_\infty = f_0$. Consequently a function $f(r)$ which is constant for 10 Å $< r <$ *ca.* 30 Å will agree with the experiments for water droplets in mixtures of 2-methyl-2-propanol and benzene, or in mixtures of 1-butanol and benzene. The upper end of the interval was found to be at least 31 Å and 23 Å, respectively, for mixtures of compositions close to the critical miscibility point. As the two coexisting liquid phases become identical at the critical point the orienting forces are extremely small in this region.

As we know that $\sigma_0/\sigma_\infty \to 1$ for $r \to \infty$ we conclude that somewhere between $r = 23$—30 Å and $r = \infty$ the value of σ/σ_∞ changes from f_0 to 1. Fig. 23 shows sketches of the two simplest ways this may happen, either (a) as a simple step function, or (b) as a gradual change-over from one asymptote to another asymptote. The transition of the interfacial tension from one value ($\sigma_0 \equiv f_0\,\sigma_\infty$) to another value ($\sigma_\infty$) with change of radius in a medium of constant composition must be connected with some change in composition or structure of the droplet. Maybe water close to a plane interface has a more regular (ice-like?) low Gibbs-energy structure, which is not stable in very small droplets.

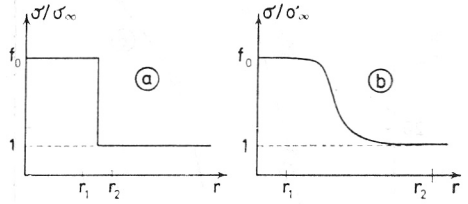

Fig. 23. Sketches of two possible ways the ratio $f \equiv \sigma/\sigma_\infty$ may depend on the radius of curvature in droplets of hydrogen bonding liquids. The experiments do not allow us to decide between the two possibilities shown as the range $[r_1; r_2]$ where the change-over takes place is not experimentally accessible.

The assumptions that

(*a*) σ is the product of a function of r and a function of c (eq. 70) and

(*b*) that the function of r is of one of the types of Fig. 23

are not sufficient for securring that σ_a/σ_∞ is a constant. We must add the assumption that

(*c*) when the composition of the ternary liquid system is changed, σ_0 and σ_∞ change, but their ratio is constant.

We are not able to explain this.

In case σ/σ_∞ depends on r as any of the functions show in Fig. 23, the classical equations apply for ΔG^* and r^*, with the value σ_0 for the interfacial tension. As the droplets nucleate they are »born« with the kind of structure that corresponds to the value σ_0, and do not »know« that they are going to get another structure (at least close to the interface) when r gets larger than a certain value.

In the systems where the precipitate is (mainly) octanol, or 2,4-dichlorophenol, σ_a/σ_∞ increases very strongly as the composition approaches that of the critical miscibility point. The high values of σ_a/σ_∞ cannot be explained by a Tolman-type of dependence on radius (with a high negative values of δ) or with the exponential type $f_e = e^{a/r}$, because the maximum value of σ_a/σ_∞ for those functions are 1.6 and 2.4, respectively.

A dependence of the type of equation (63) where σ/σ_∞ is put equal to $1 + a/r$ allows for unlimited high values of σ_a/σ_∞. For $a/r \to \infty$ we have $f \to \infty$ and (from equations 66 and 68)

$$\frac{\sigma_a}{\sigma_\infty} \approx 2^{-1/3} f = 0.7936 \cdot f \tag{72}$$

$$\frac{r}{r_a} \to 2^{-2/3} = 0.6300 \tag{73}$$

From this follows that for large values of f (say $f > 10$) we have

$$a = (f - 1)\, r \approx 2^{1/3} (\sigma_a/\sigma_\infty)\, r \approx 2^{-1/3} (\sigma_a/\sigma_\infty)\, r_a \tag{74}$$

In the series of experiments with 2,4-dichlorophenol and with octanoic acid both σ_a/σ_∞ an r_a increase as the composition moves towards critical miscibility (decreasing water volume fraction). Therefore the parameter a, which is close to the product of these factors will also vary. The accurate calculations, using equations (66), (68), and (63) give in the case of 2,4-dichlorophenol, $a = 27.0$ Å at $r_a = 13.23$ Å ($r = 11.5$ Å) and $a = 3680$ Å at $r = 48.7$ Å ($r_a = 76.3$ Å). For octanoic acid we find similarly, $a = 4.7$ Å at $r_a = 9.8$ Å ($r = 7.0$ Å) and $a = 4220$ Å at $r_a = 48.8$ Å ($r = 30.8$ Å).

We conclude that the experiments cannot be accounted for by an expression like equation (70) with $f(r) = 1 + a/r$. Trials with other functions $f(r)$ did not lead to any essentially better agreement. For any function of the general type

$$\sigma/\sigma_\infty \equiv f_n(r) \equiv (1 + a/r)^p \tag{75}$$

we find

$$\sigma_a/\sigma_\infty = (1 + a/r)^{p-1} [\{1 + (1 - p/2)\,(a/r)\}^2 \{1 + (1 + p)\,(a/r)\}]^{1/3} \tag{76}$$

$$\frac{r}{r_a} = \left[\frac{1 + (1 - p/2)\,(a/r)}{1 + (1 + p)\,(a/r)}\right]^{1/3} \tag{77}$$

For $a/r \to \infty$ we have

$$\sigma/\sigma_\infty \equiv f \approx (a/r)^p \to \infty \tag{78}$$

$$\sigma_a/\sigma_\infty \approx \begin{cases} [(1 - p/2)^2\,(1 + p)]^{1/3}\,(a/r)^p \to \infty & (p \neq 2) \\ 3^{1/3}\,(a/r)^{1/3} \to \infty & (p = 2) \end{cases} \tag{79}$$

$$\frac{r}{r_a} \longrightarrow \left[\frac{1 - p/2}{1 + p}\right]^{1/3} \tag{80}$$

For large values of f we have

$$\sigma_a/\sigma_\infty \approx \begin{cases} \left[\left(1 - \frac{p}{2}\right)^2 (1 + p)\right]^{1/3} \sigma/\sigma_\infty & (p \neq 2) \\ 3^{1/3}\,(\sigma/\sigma_\infty)^{2/3} & (p = 2) \end{cases} \tag{81}$$

$$r/r_a \longrightarrow \text{a constant} \begin{cases} \neq 0 \text{ for } p \neq 2 \\ = 0 \text{ for } p = 2 \end{cases} \tag{82}$$

For all $p > 0$ (except for $p = 2$) the conclusion will be the same as derived for $f_1 = 1 + a/r$ (*i. e.* for $p = 1$).

In the singular case of $p = 2$, r/r_a goes to zero as the composition approaches the critical miscibility point. Application to the experimental data gives extremely small values of r, less than a molecular radius. So we may conclude that none of the possibilities of eq. (75) apply to our empirical data.

We notice that a dependence of σ/σ_∞ on r of the type shown in Fig. 23 will be able to explain our results with 2,4-dichlorophenol and with octanoic acid. The difference between the two systems with these precipitates, and the systems with water as the precipitate would be that there is no proportionality between σ_0 and σ_∞ as the composition is varied in either of the systems with dichlorophenol and octanoic acid. In stead σ_∞ wil go faster to zero than σ_0, as the critical miscibility point is approached, so that σ_0/σ_∞ reaches very large values. We cannot see any reason for denying the possibility that σ_0/σ_∞ goes to infinity as $\sigma_\infty \rightarrow 0$.

It is tempting to speculate on the cause of the distinct difference between the two kinds of behaviour. The change-over between two values of σ (σ_0 and σ_∞) is assumed to correspond to changes in the structure. In the case of water droplets we could imagine that the structure at a flat interface is icelike, and at a curved interface (with water inside) it is more irregular, perhaps like in the interior of a macroscopic water phase.

For a droplet of dichlorophenol or octanoic acid situated in a mixture of methanol and water, we should expect the molecules in the surfaces to try to orient themselves with the hydrophilic group in the methanol-water-phase and the hydrophobic part of the molecules in the oily droplet phase. Such a micellar structure will be more stable than a structure with random orientation, if it leads to a true oily (hydrophobic) milieu inside the droplet, and if there is space enough inside the droplet for all the hydrophobic parts of the molecules in the surface of the droplet. For very small droplets this is not the case. The micellar or ordered-layer structures is therefore not possible at very small radii. This explains that the structure of the interface changes at a certain value of radius. In the small droplets the random orientation of the molecules typical for the interior of a normal liquid is extended to include the molecules in the surface. If *e. g.* 90% of the surface of a single molecule is hydrophobic, then 90% of the surface of a droplet with randomly oriented molecules will be hydrophobic and only 10% will be hydrophilic. The value of σ_0 will therefore be very close to that of a 100% hydrophobic substance. This is just what we have found. For the molecules without hydrogen bonding groups studied here the interfacial tension against almost pure water is of the order, 25 to 35 mJ/m^2, (see Fig. 15—17). For molecules having a hydrogen bonding group the interfacial tension against water is considerably lower (5 to 7 mJ/m^2 in Fig. 18 and 19, respectively). But σ_0 is close to the value for a nonhydrogen bonding liquid. (15 and 28 mJ/m^2 for 2,4-dichlorophenol and octanoic acid, respectively).

CONCLUSION

Concerning nucleation in the eight ternary liquid systems with miscibility gap studied so far (the seven systems of the present paper and tribromomethane--methanol-water[17]) we may conclude:

1. When the supersaturation is chosen so high that the liquid becomes strongly turbid in about one millisecond, the relation between the supersatu-

ration and the induction period agrees with the assumption of homogeneous nucleation followed by diffusion controlled growth of spherical droplets.

2. According to the interfacial tensions calculated under the assumption of the mechanism of (1) the systems fall into three classes.

a) The precipitate consists mainly of a non hydrogen bonding liquid (polar or nonpolar). The interfacial tension calculated from nucleation experiments is identical with the macroscopic (plane interface) value obtained by a classical method (*i. e.* the drop weight method), or it varies a little with the droplet radius according to Tolman's equation with a positive or negative δ, which is of the same order of magnitude as the molecular diameter.

b) The precipitate consists mainly of water. The ratio σ/σ_∞ between the nucleation and the macroscopic interfacial tension is constant, of the order of 5 to 10. This behaviour would be expected if the dependence of σ on r for constant composition of the surrounding medium shows two regions of constant σ ($\sigma = \sigma_0$ at $r < r_1$ and $\sigma = \sigma_\infty$ *at* $r > r_2$). The transition interval was not located more precisely than can be expressed by stating that $r_1 > 23$ Å or 31 Å, for the two systems respectively. At the same time, σ_0/σ_∞ must be independent of the composition of the ternary system.

c) The precipitate consists mainly of organic molecules which are sparingly soluble in water, but which have one hydrophilic, hydrogen bonding group. The ratio σ/σ_∞ increases with increasing radius of the spherical droplet. This behaviour could not be explained by assuming gradual change of σ/σ_∞ with r of any of the types, $\sigma/\sigma_\infty = 1/(1 - a/r)$; $e^{a/r}$; or $(1 + a/r)^p$ $(p > o)$. But it could be explained by the same kind of dependence of σ on r as in (b) if the ratio σ_0/σ_∞ is not constant but increases (to values of the order of one hundred or more, when the composition of the system approaches the critical solubility point, *i. e.* when σ_0 and σ_∞ both go to zero.

The conclusions are very similar to the conclusions of Abraham[10-13] on the dependence of σ on droplet size in supersaturated vapours condensing to droplets.

REFERENCES

1. J. W. Gibbs, *The Scientific Papers* (1906) Dover, New York 1961, **1** 219.
2. R. C. Tolman, *J. Chem. Phys.* **16** (1948) 758; **17** (1949) 118, 333.
3. F. O. Koenig, *J. Chem. Phys.* **18** (1950) 449.
4. J. G. Kirkwood and F. P. Buff, *J. Chem. Phys.* **17** (1949) 338; **18** (1950) 991.
5. F. P. Buff, *J. Chem. Phys.* **19** (1951) 1591; **23** (1955) 419.
6. T. L. Hill, *J. Chem. Phys.* **36** (1962) 3182.
7. S. Kondo, *J. Chem. Phys.* **25** (1956) 662.
8. S. Ono and S. Kondo, *Handbuch der Physik* **10** (1960).
9. D. S. Choi, M. S. Jhon, and H. Eyring, *J. Chem. Phys.* **53** (1970) 2608.
10. F. F. Abraham, *Appl. Phys. Lett.* **13** (1968) 208.
11. F. F. Abraham, *J. Appl. Phys.* **39** (1968) 5811.
12. F. F Abraham, *J. Chem. Phys.* **50** (1969) 3977.
13. F. F. Abraham, *Science* **168** (1970) 833.
14. J.-Y. Parlange, *J. Crystal Growth* **6** (1970) 311.
15. A. E. Nielsen, *Kinetics of Precipitation,* Oxford, New York, 1964.
16. A. E. Nielsen, *Kristall und Technik* **4** (1969) 17.
17. A. E. Nielsen and S. Sarig, *J. Crystal Growth* **8** (1971) 1.
18. A. E. Nielsen and O. Söhnel, *J. Crystal Growth* **11** (1971) 233.
19. D. R. White and J. L. Kassner, *J. Colloid Interface Sci.* **39** (1972) 59.
20. R. J. Good, *J. Phys. Chem.* **61** (1957) 810.

21. J. H. Hildebrand, *J. Am. Chem. Soc.* **51** (1929) 66; **57** (1935) 866.
22. J. H. Hildebrand and R. L. Scott, *The Solubility of Nonelectrolytes*, 1924, Dover, New York, 1964, 121.
23. J. H. Hildebrand, J. M. Prausnitz, and R. L. Scott, *Regular and Related Solutions*, New York, 1970.

IZVOD

Utjecaj zakrivljenosti na površinsku napetost tekućih sistema mjerenih homogenom nukleacijom

A. E. Nielsen i P. S. Bindra

Mjerene su površinske napetosti ternarnih tekućih sistema koji se sastoje iz dviju faza nastalih nukleacijom kapi iz homogene otopine. Ternarni sistem sastojao se iz dvaju otapala i u njima jedne netopljive komponente. Kada je ta posljednja tekućina koja ne tvori vodikove veze, površinska je napetost neovisna o zakrivljenosti površine i po veličini je identična s makroskopski mjerenom napetosti. Ako se kapi sastoje od vode koja se miješanjem dvaju otapala izdvaja iz jednog od njih, odnos promatrane je prema mikroskopskoj napetosti površine između 5 i 10. Konačno, ako se kapi stvaraju od organskih molekula slabo topljivih u vodi, ali koje imaju jednu hidrofilnu skupinu koja tvori vodikove veze, tada je napetost površine neka nepredskaziva funkcija polumjera kapi.

MEDICINSK-KEMISK INSTITUT
UNIVERSITY OF COPENHAGEN
COPENHAGEN, DENMARK

Primljeno 27. studenoga 1972.